Representing perturbed dynamics in biological network models

Gautier Stoll,[1,3,*] Jacques Rougemont,[3,†] and Felix Naef[1,2,3,‡]
[1]*NCCR Molecular Oncology, chemin des Boveresses 155, 1066 Epalinges, Switzerland*
[2]*School of Life Sciences, ISREC, Ecole polytechnique Fédérale de Lausanne 1015 Lausanne, Switzerland*
[3]*Swiss Institute of Bioinformatics, Quartier Sorge-Genopode, 1015 Lausanne, Switzerland*
(Received 28 February 2007; published 25 July 2007)

We study the dynamics of gene activities in relatively small size biological networks (up to a few tens of nodes), e.g., the activities of cell-cycle proteins during the mitotic cell-cycle progression. Using the framework of deterministic discrete dynamical models, we characterize the dynamical modifications in response to structural perturbations in the network connectivities. In particular, we focus on how perturbations affect the set of fixed points and sizes of the basins of attraction. Our approach uses two analytical measures: the basin entropy H and the perturbation size Δ, a quantity that reflects the distance between the set of fixed points of the perturbed network and that of the unperturbed network. Applying our approach to the yeast-cell-cycle network introduced by Li *et al.* [Proc. Natl. Acad. Sci. U.S.A. **101**, 4781 (2004)] provides a low-dimensional and informative fingerprint of network behavior under large classes of perturbations. We identify interactions that are crucial for proper network function, and also pinpoint functionally redundant network connections. Selected perturbations exemplify the breadth of dynamical responses in this cell-cycle model.

DOI: 10.1103/PhysRevE.76.011917 PACS number(s): 87.16.Yc, 87.80.Vt

I. INTRODUCTION

Recent experimental developments in the fields of genomics, e.g., whole genome DNA sequencing or proteomics, are opening possibilities for systems level studies in biology [1–4]. In particular, the notion that biological functions may rely on a large number of interconnected variables (for example, genes) working in concert has stimulated general theoretical interest about properties of biological networks [5]. Studies of the statistical properties of large (typically thousands of nodes) biological networks have identified a number of functional building blocks, termed network motifs, that occur more frequently than random [6]. These findings support the idea that some systems are designed around a modular architecture in which autonomous modules are wired together to generate versatile biological functions [1,4,7,17]. While structural (or topological) properties are key for network characterization, functional properties are ultimately encoded in dynamical or time-dependent changes in the state variables of the nodes. The sizes of systems that can be modeled dynamically are typically much smaller (10–100 nodes). One common modeling approach, for example for the yeast cell cycle [9], is to simulate the nonlinear system of chemical rate equations describing the putative biochemical processes. Modeling approaches have been applied to a number of systems, including the cell cycle [9,10], and the λ-phage switch in *Escherichia coli* [8]. Although these models provide a detailed description, this approach suffers from the caveat that most parameters are currently not accessible experimentally. In addition, the number of parameters is typically about five per reaction, resulting in a prohibitively large parameter space. This last point makes it difficult to grasp the full solution space of the model. Recent approaches based on sampling the parameter space in optimal regions have been developed [11]. At the opposite end of model complexity, dynamical rules based on Boolean state variables have been useful for studying more global dynamical properties of topological classes of networks [12,13]. In addition, Boolean models have been successfully applied to the yeast cell cycle [14,18] and the body patterning in drosophila embryos [15,16].

In this study, we develop a systematic approach to describe how the dynamical landscape of small (less than about 50 nodes) Boolean networks is affected by perturbations in the network connectivity. In particular, we consider the basin entropy H, a quantity that considers the size distribution of the basins of attraction. We complement the entropy with a measure of distance between the stable fixed points of a perturbed network and those in the unperturbed network. This combination gives a low-dimensional and compact representation of the patterns induced by a large number of perturbations. We illustrate our methods using the yeast-cell-cycle network introduced in [14], and discuss examples of structural perturbations producing a range of modified basins of attraction.

II. DEFINITIONS

Following [14] a network of N nodes can be represented by an $N \times N$ adjacency matrix A, in which an activating link between node i and node j is represented by $A_{ij}=1$ and an inhibiting link by $A_{ij}=-1$. The possibility of self-inhibitory (or activating links) $A_{ii}=\pm 1$ is not excluded. In the Boolean approximation, each node has two possible states, so that the global state of all nodes can be represented by a vector $\mathbf{S}$, with $S_i=1$ when the node i is on and $S_i=0$ if the node is off. The full phase space containing 2^N states is denoted by Λ.

A. Boolean dynamics

A simple dynamical rule that characterizes the temporal evolution of the state variable can be defined following [14],

*Gautier.stoll@curie.fr
†jacques.rougemont@isb-sib.ch
‡felix.naef@isrec.ch

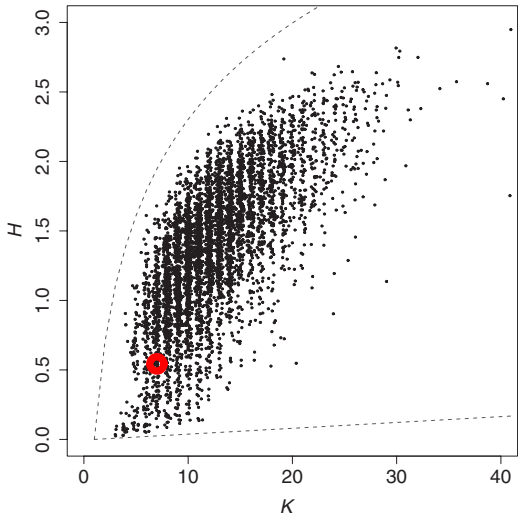

FIG. 1. (Color online) Entropy vs number of attractors after class I perturbation (shuffled arrows). The range of possible H values is indicated by the dashed gray lines. The plain circle [red (gray)] represents the reference network; the other points show the perturbed networks.

which is closely related to update rules applied in perceptron models. If the network is in the state $\mathbf{S}(t)$ at time t, the state at the next time step $\mathbf{S}(t+1)$ is given by

$$S_i(t+1) = \begin{cases} 1 & \text{if } \sum_j A_{ij} S_j(t) > 0, \\ S_i(t) & \text{if } \sum_j A_{ij} S_j(t) = 0, \\ 0 & \text{if } \sum_j A_{ij} S_j(t) < 0. \end{cases} \quad (1)$$

For a given network, we apply this rule to every possible initial condition in Λ. This defines orbits (trajectories) that must end in a limit cycle (periodic attractor) since we are dealing with a dynamical system on a finite space. A fixed point is a cycle of length 1.

Accordingly, Λ can be decomposed into a disjoint union of K basins of attraction B_k of size d_k: $\Lambda = \cup_{k=1}^{K} B_k$.

In a biological network, the attractors correspond to functional end points, and it is important that the states in the attractors are consistent with observed data. For example, by far the largest end point in the cell-cycle network of Li *et al.* (see the Appendix) corresponds to the stationary G1 phase in the cycle. Other systems are more switchlike, for instance in signal transduction, where a cell might change its state from growth to differentiation according to an external trigger. To characterize these attractors, we introduce the following definitions.

(a) We compute the *number of attractors* K: an attractor is a limit cycle or a fixed point. An attractor A has a basin of attraction B which is the set of all initial conditions whose orbit converges to A.

(b) The *basin entropy* H is defined as follows. Let $p_k = 2^{-N} d_k$ be the probability that an initial state belongs to basin B_k. Then the entropy reads

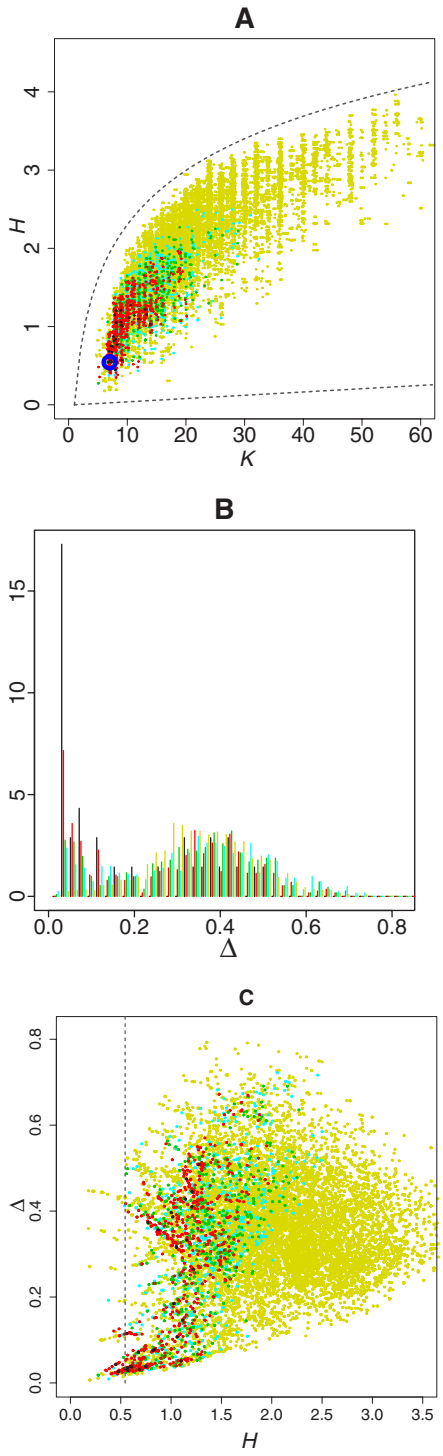

FIG. 2. (Color online) Entropy, number of attractors, and Δ after class II perturbations (removed arrows). Colors (or gray shades) represent different numbers of removed arrows: Color version: black for one removed arrows, red for two, green for three, turquoise for four, and yellow for more than four. Black and white version: black for one removed arrow, dark gray for two and three, light gray for more than three. (a) Entropy H vs number of basins K for class II perturbations. The range of possible H values is indicated by the dashed gray lines, the open blue (gray) circle (located in the lower left corner) represent the reference network. (b) Distribution of Δ shows bimodal behavior. (c) Δ vs H plot; the dashed gray line represents the entropy of the reference network.

TABLE I. Basins of attraction with their respective probabilities (in %, last column) for the original YCC network. The boolean entries represent the state of the gene indicated in the column heading. The largest basin ends at the G1 stationary state. Entropy $H=0.543$, number of attractors $K=7$.

Cln3	MBF	SBF	Cln1,2	Cdh1	Swi5	Cdc20,14	Clb5,6	Sic1	Clb1,2	Mcm1	%
0	0	0	0	1	0	0	0	1	0	0	0.8613
0	0	1	1	0	0	0	0	0	0	0	0.0737
0	1	0	0	1	0	0	0	1	0	0	0.0532
0	0	0	0	0	0	0	0	1	0	0	0.0043
0	0	0	0	0	0	0	0	0	0	0	0.0034
0	1	0	0	0	0	0	0	1	0	0	0.0034
0	0	0	0	1	0	0	0	0	0	0	0.0004

$$H := -\sum_{k=1}^{K} p_k \log(p_k). \tag{2}$$

H is maximum $[H=\log(K)]$ if each state is its own basin of size 1, and minimum $(H=0)$ when there is one single basin. H is a natural measure for characterizing basin structures [19]. Because it takes into account the relative basin sizes, it is quite insensitive to the appearance of small and biologically irrelevant basins.

(c) The *perturbation size* Δ measures the distance between attractors of a perturbed and a reference network: from each initial condition, the Hamming distance between the fixed points is computed, and the average over all initial conditions is taken. More precisely, if $\mathbf{F}_G(\mathbf{S})$ is the fixed point of the trajectory starting at $\mathbf{S}$ and generated by the network G, then

$$\Delta_{G,G'} := \frac{1}{2^N}\sum_{\mathbf{S}} \delta(\mathbf{F}_G(\mathbf{S}),\mathbf{F}_{G'}(\mathbf{S})) \tag{3}$$

where $\delta(\cdot,\cdot)$ is the Hamming distance between two Boolean states, namely,

$$\delta(\mathbf{S},\mathbf{T}) := \frac{1}{N}\sum_{i} |S_i - T_i|. \tag{4}$$

The value Δ has the following interpretation: it is the average probability (taken over all nodes) that, for a random initial condition, the final state of a node differs. In this study, the reference network G will be the cell-cycle network of Li *et al.*, which has one very large basin of attraction and several smaller ones. If some trajectories in the perturbed networks G' end in a limit cycle, Δ is defined as the average of the Hamming distance along the cycle.

B. Network models and perturbations

Our goal is to assess how network dynamics is affected by several types of perturbations. We consider two classes. One of them randomizes the adjacency matrix while keeping invariant a number of topological characteristics from the original network. The second class mimics biological perturbations, as would occur, for example, through mutations in the interaction partners that constitute the network links. The two classes are defined as follows.

(a) *Shuffle* (class I): all activating and inhibiting arrows are cut in half and rewired randomly. This ensures that the connectivity at each node is conserved. As compared to the Li *et al.* study [14], we generate random networks that are more constrained, since the connectivity at each node is forced to remain unchanged after randomization. Such perturbations are applied in the studies of network motifs [4,6].

(b) *Remove* (class II): the arrows are simply suppressed. We extend this class of perturbations beyond single-link removal.

TABLE II. Basins of attraction with their respective probabilities when (Cdc20,Cdc14)→Clb1,2 and Sic1→Clb1,2 are removed. Entropy=0.549, number of attractors=9, $\Delta=0.41$.

Cln3	MBF	SBF	Cln1,2	Cdh1	Swi5	Cdc20,14	Clb5,6	Sic1	Clb1,2	Mcm1	%
0	0	0	0	0	1	1	0	1	1	1	0.880
0	0	0	0	1	0	0	0	1	0	0	0.054
0	0	1	1	0	0	0	0	0	0	0	0.027
0	1	0	0	1	0	0	0	1	0	0	0.015
0	0	0	0	1	1	1	0	1	1	1	0.010
0	0	0	0	0	0	0	0	1	0	0	0.004
0	0	0	0	0	0	0	0	0	0	0	0.003
0	1	0	0	0	0	0	0	1	0	0	0.003
0	0	0	0	1	0	0	0	0	0	0	0.000

TABLE III. Basins of attraction with their respective probabilities when SBF→Cln1,2 is removed. Entropy $H=1.096$, number of attractors $K=12$, $\Delta=0.05$.

Cln3	MBF	SBF	Cln1,2	Cdh1	Swi5	Cdc20,14	Clb5,6	Sic1	Clb1,2	Mcm1	%
0	0	0	0	1	0	0	0	1	0	0	0.6669
0	1	1	0	1	0	0	0	1	0	0	0.1762
0	0	1	0	1	0	0	0	1	0	0	0.0654
0	1	0	0	1	0	0	0	1	0	0	0.0532
0	1	1	0	0	0	0	0	1	0	0	0.0180
0	0	1	0	0	0	0	0	1	0	0	0.0043
0	0	0	0	0	0	0	0	1	0	0	0.0043
0	0	0	0	0	0	0	0	0	0	0	0.0034
0	0	1	0	0	0	0	0	0	0	0	0.0034
0	1	0	0	0	0	0	0	1	0	0	0.0034
0	0	0	0	1	0	0	0	0	0	0	0.0004
0	0	1	0	1	0	0	0	0	0	0	0.0004

III. RESULTS

We study the yeast-cell-cycle (YCC) network of Li *et al.* [14], in which a Boolean model reproducing the different phases of the cycle is constructed (see the Appendix). This model has a main fixed point attracting 86% of the initial conditions. Biologically this state corresponds to the G1 stationary phase of the cell cycle, as reflected by the activities of the respective nodes. Using computer simulations, the authors further showed that the cell-cycle dynamics had certain robustness properties when challenged with perturbations. In particular, it was shown that, in a majority of cases, removal of one link or addition of a link at random did not change much the size of the largest basin of attraction. Finally, the studied network had unusual trajectory channeling properties, when compared to random networks with equal numbers of nodes and links. Here we extend the characterization of this model by introducing a combination of measures to characterize the structure of basins of attraction as they are modified by structural perturbations. In particular we investigate the consequences of combined mutations and show that they can lead to a cancellation effect.

A. Study of shuffled networks (class I perturbations)

This type of perturbation allows us to study the dynamical characteristics of a biological network in comparison with random networks belonging to a topological class. Figure 1 shows the number of attractors (K) and the entropy (H) of the YCC network and randomly shuffled (class I) versions thereof.

The location of the reference network in the $H-K$ plane with respect to the scatter of the perturbed networks allows us to assess how typically a network behaves with respect to a class. Accordingly, the YCC network is atypical, as seen by its marginal location in the lower left corner. Indeed, this network has lower entropy and fewer basins than most networks, consistent with [14].

B. Study of mutated networks (class II perturbations)

The previous discussion shows how entropy characterizes the system of attractors. However, H contains only information about the relative weights of the attractors, irrespective of their biological relevance. For example a perturbation can decrease the entropy while shifting the fixed point away from that in the unperturbed, biologically relevant state. For this reason we introduced a second quantity Δ [Eq. (3)], a probabilistic measure of the change in the fixed point after perturbation. The quantities H and Δ are independent and probe two separate effects of a perturbation: H tells if the structure of basins is more ($\delta H=H-H_0>0$) or less ($\delta H<0$) frag-

TABLE IV. Basins of attraction with their respective probabilities when (Cdc20,Cdc14)→Clb1,2, Clb1,2→Mcm1, Clb1,2→Cdh1 and Clb1,2→Swi5 are removed. Entropy $H=0.523$, number of attractors $K=7$, $\Delta=0.025$.

Cln3	MBF	SBF	Cln1,2	Cdh1	Swi5	Cdc20,14	Clb5,6	Sic1	Clb1,2	Mcm1	%
0	0	0	0	1	0	0	0	1	0	0	0.8793
0	0	1	1	0	0	0	0	0	0	0	0.0507
0	1	0	0	1	0	0	0	1	0	0	0.0356
0	0	0	0	0	0	0	0	1	0	0	0.0268
0	1	0	0	0	0	0	0	1	0	0	0.0034
0	0	0	0	0	0	0	0	0	0	0	0.0034
0	0	0	0	1	0	0	0	0	0	0	0.0004

TABLE V. Adjacency matrix of the yeast-cell-cycle network. The numbers refer to the ordering of the nodes as used in Tables I–IV and VI + (−) represent activating (repressing) links.

$1\overset{+}{\rightarrow}2$	$1\overset{+}{\rightarrow}3$	$2\overset{+}{\rightarrow}8$	$3\overset{+}{\rightarrow}4$	$6\overset{+}{\rightarrow}9$	$7\overset{+}{\rightarrow}5$	$7\overset{+}{\rightarrow}6$	$7\overset{+}{\rightarrow}9$	$8\overset{+}{\rightarrow}10$	$8\overset{+}{\rightarrow}11$	$10\overset{+}{\rightarrow}7$	$10\overset{+}{\rightarrow}11$
$11\overset{+}{\rightarrow}6$	$11\overset{+}{\rightarrow}7$	$11\overset{+}{\rightarrow}10$	$4\overset{-}{\rightarrow}9$	$4\overset{-}{\rightarrow}5$	$5\overset{-}{\rightarrow}10$	$7\overset{-}{\rightarrow}8$	$7\overset{-}{\rightarrow}10$	$8\overset{-}{\rightarrow}5$	$8\overset{-}{\rightarrow}9$	$9\overset{-}{\rightarrow}8$	$9\overset{-}{\rightarrow}10$
$10\overset{-}{\rightarrow}2$	$10\overset{-}{\rightarrow}3$	$10\overset{-}{\rightarrow}5$	$10\overset{-}{\rightarrow}6$	$10\overset{-}{\rightarrow}9$	$1\overset{-}{\rightarrow}1$	$4\overset{-}{\rightarrow}4$	$6\overset{-}{\rightarrow}6$	$7\overset{-}{\rightarrow}7$	$11\overset{-}{\rightarrow}11$		

mented, with H_0 the entropy of the reference network, while Δ measures the distance between perturbed and reference attractors (see the definitions above).

We first repeat Fig. 1 for class II perturbations, which shows that networks with only few perturbations cluster around the wild-type model [Fig. 2(a)], while the spread for networks with four perturbations resembles the shuffled models (Fig. 1). Turning to the measure of Δ, we find that the Δ distribution [Fig. 2(b)] is bimodal, showing two distinct populations of perturbations ($\Delta \lesssim 0.2$ and $\Delta \gtrsim 0.2$). In the second case the perturbed model does not follow the canonical cell-cycle progression, and thus has fixed points that do not characterize the wild-type situation. Nevertheless, a low entropy H would indicate a large main basin of attraction around that new fixed point. However, when Δ is small, the system of attractors of the perturbed network is consistent with the biological reference, and the entropy ΔH allows us to distinguish between networks with a larger or smaller main basin of attraction. Thus the entropy and Δ are complementary for describing the dynamical changes induced by a large set of perturbations [Fig. 2(c)]. The two modes in the Δ istogram are clearly reflected on this two-dimensional representation. Noticeably, Δ spans a broad range for any number of removed arrows, meaning that few (one or two) removed arrows can already change the fixed points significantly. In contrast, higher entropies are far more frequent when a large number (>2) of arrows are removed, indicating that several mutations are necessary to strongly fragment the basin structure.

In summary, the distribution of Δ conveys a measure of network *robustness*. Accordingly, the present network is not very robust since relatively mild perturbations (fewer than two removed arrows) can induce large Δ [Figs. 2(b) and 2(c)]. The main characteristic of H, which appears independent of Δ, is that a few removed links (one or two) preserves the entropy within one unit (in natural logarithm ~ 1.4 bits). In this range basins remain relatively compact even when they do not represent the wild-type cell cycle. Keeping biological function in mind, H will be most relevant when Δ is small, as we now explain.

The different locations in the H-Δ plane have the following interpretations.

(1) If Δ is large ($\Delta \gtrsim 0.2$), the model does have attractor states which do not coincide with the gene activities of the different cell-cycle phases. Such perturbations are especially interesting if the number of removed arrows is small (dark colors). Such links are then essential for the model, as their removal severely disrupts the cell cycle.

(2) If Δ is small and the entropy increases, the probability that the dynamics ends in the reference attractor decreases, demonstrating that the removed arrows contributed to the channeling properties of the system.

(3) If Δ is small and the entropy decreases, the main attractor of the perturbed network has a stronger attraction property. Some of these networks could be considered as alternative cell-cycle models.

C. Examples of mutations

We illustrate the above three regimes. For reference, the attractor sizes in the unperturbed model are listed in Table I. In the first example (Table II), we find a large main basin of attraction as in the unperturbed model. However, the fixed point is significantly different from that of the wild type as the system is blocked in a state of the M phase and cannot finish the cell cycle properly (see the Appendix for the recapitulation of the wild-type mode from [14]).

In the second example (Table III), the dynamics has the same main fixed point as the wild type, but with a smaller basin of attraction, while the second biggest has grown. Therefore the removed connection $\mathrm{SBF}\rightarrow\mathrm{Cln1,2}$ contributes to the ability of the main fixed point to funnel trajectories.

The third example (Table IV) is a model with four removed arrows which has the same main fixed point with a slightly higher probability. Also, the second largest fixed point is the same as in the wild-type model. This indicates that the effect of some mutations can be canceled by further mutations. While such cases exist, we found that networks with several removed links that preserve the unperturbed cell-cycle behavior are rare.

IV. CONCLUSION

We have proposed a systematic approach for studying the dynamical attractor landscape of biological networks, and their response to structural perturbations. In particular, we introduced a low-dimensional representation of the system of attractors, the entropy, and a probabilistic measure in the perturbation size, Δ. This enabled us to study the global characteristics of network perturbation in a compact and visually effective form. In a biological context, this can provide hints to elucidate the dynamical role of specific network links. Alternatively, the functions of new and yet unobserved links can be predicted as in [18], and imperfect starting models can be improved.

We applied this method to a model of the yeast cell cycle by Li *et al.* Using the measures introduced, we generalized the dynamical characterization of the model using a broad range of perturbations. This enabled us to emphasize the

TABLE VI. Discrete time evolution of the Boolean states of the YCC network as it traverses the different cell-cycle phases. Cdc20.14 has been abbreviated C20,14; G1* indicates the stationary G1 phase.

t	Cln3	MBF	SBF	Cln1,2	Cdh1	Swi5	C20,14	Clb5,6	Sic1	Clb1,2	Mcm1	Phase
1	1	0	0	0	1	0	0	0	1	0	0	START
2	0	1	1	0	1	0	0	0	1	0	0	G1
3	0	1	1	1	1	0	0	0	1	0	0	G1
4	0	1	1	1	0	0	0	0	0	0	0	G1
5	0	1	1	1	0	0	0	1	0	0	0	S
6	0	1	1	1	0	0	0	1	0	1	1	G2
7	0	0	0	1	0	0	1	1	0	1	1	M
8	0	0	0	0	0	1	1	0	0	1	1	M
9	0	0	0	0	0	1	1	0	1	1	1	M
10	0	0	0	0	0	1	1	0	1	0	1	M
11	0	0	0	0	1	1	1	0	1	0	0	M
12	0	0	0	0	1	1	0	0	1	0	0	G1
13	0	0	0	0	1	0	0	0	1	0	0	G1*

breadth of dynamical behavior (Fig. 2) induced by only few mutated links. Interestingly, we observed [Fig. 2(c)] that the structure of the system of attractors (H) behaves quite robustly compared to the modification in the final states (Δ), especially when the number of removed links is small (<3). We illustrated through examples the consequences of removing individual or groups of links. Interestingly it was possible to remove up to four links while not affecting the basin structure significantly. Tracking the dynamical changes in the activity levels of a proteins in a network is a very high-dimensional problem. It is therefore important to have few informative variables which allow one to efficiently assess a large number of perturbed models at once. We believe that the basin entropy and distance to a reference attractor are well suited for this purpose.

ACKNOWLEDGMENTS

We thank the organizers of the CompBioNets '04 conference (Recife, Brazil) at which an initial version of this work was presented. The simulations were performed on an Itanium2 cluster from HP/Intel at the Vital-IT facilities. F.N. and G.S. acknowledge funding from the NCCR Molecular Oncology program and the NIH administrative supplement to parent Grant No. GM54339.

APPENDIX: THE YEAST-CELL-CYCLE NETWORK OF LI *et al.*

Tables V and VI are recapitulated from [14].

[1] L. H. Hartwell, J. J. Hopfield, S. Leibler, and A. W. Murray, Nature (London) **402**, C47 (1999).
[2] E. Alm and A. P. Arkin, Curr. Opin. Struct. Biol. **13**, 193 (2003).
[3] Z. N. Oltvai and A. L. Barabasi, Science **298**, 763 (2002).
[4] U. Alon, Science **301**, 1866 (2003).
[5] A. L. Barabasi and Z. N. Oltvai, Nat. Rev. Genet. **5**, 101 (2004).
[6] R. Milo, S. Shen-Orr, S. Itzkovitz, N. Kashtan, D. Chklovskii, and U. Alon, Science **298**, 824 (2002).
[7] J. Ihmels, G. Friedlander, S. Bergmann, O. Sarig, Y. Ziv, and N. Barkai, Nat. Genet. **31**, 370 (2002).
[8] A. Arkin, J. Ross, and H. H. McAdams, Genetics **149**, 1633 (1998).
[9] B. Novak, A. Csikasz-Nagy, B. Gyorffy, K. Chen, and J. J. Tyson, Biophys. Chem. **72**, 185 (1998).
[10] F. R. Cross, V. Archambault, M. Miller, and M. Klovstad, Mol. Biol. Cell **13**, 52 (2002).
[11] K. S. Brown and J. P. Sethna, Phys. Rev. E **68**, 021904 (2003).
[12] A. Aldana, S. Coppersmith, and L. P. Kadanoff, e-print arXiv:nlin-sys/0204062.
[13] S. Kauffman, C. Peterson, B. Samuelsson, and C. Troein, Proc. Natl. Acad. Sci. U.S.A. **100**, 14796. (2003).
[14] F. Li, T. Long, Y. Lu, Q. Ouyang, and C. Tang, Proc. Natl. Acad. Sci. U.S.A. **101**, 4781 (2004).
[15] R. Albert and H. G. Othmer, J. Theor. Biol. **223**, 1 (2003).
[16] M. Chaves, R. Albert, and E. D. Sontag, J. Theor. Biol. **235**, 431 (2005).
[17] A. Vazquez, R. Dobrin, D. Sergi, J.-P. Eckmann, Z. N. Oltvai, and A.-L. Barabasi, Proc. Natl. Acad. Sci. U.S.A. **101**, 17940 (2004).
[18] G. Stoll, J. Rougemont, and F. Naef, Bioinformatics **22**, 2539 (2006).
[19] T. M. Cover and J. A. Thomas, *Elements of Information Theory* (Wiley, New York, 1991).